Earth and Planetary Science Letters, 97 (1990) 113–128
Elsevier Science Publishers B.V., Amsterdam – Printed in The Netherlands

[XLeP]

Geochronology of TAG and Snakepit hydrothermal fields, Mid-Atlantic Ridge: witness to a long and complex hydrothermal history

C. Lalou [1], G. Thompson [2], M. Arnold [1], E. Brichet [1], E. Druffel [2] and P.A. Rona [3]

[1] *Centre des Faibles Radioactivités, Laboratoire mixte CNRS-CEA, 91198 Gif-sur-Yvette Cedex (France)*
[2] *Woods Hole Oceanographic Institution, Woods Hole, MA 02543 (U.S.A.)*
[3] *NOAA/AOML, 4301 Rickenbacker Causeway, Miami, FL 33149 (U.S.A.)*

Received June 12, 1989; revised version accepted October 3, 1989

Geochronological studies of a large number of precipitates from the TAG hydrothermal field and of few samples from Snakepit hydrothermal field of the Mid-Atlantic Ridge show intermittent repeated hydrothermal events at both sites. $^{210}Pb/Pb$ and $^{230}Th/^{234}U$ measurements of sulfides, iron and manganese oxides, and ^{14}C measurements of carbonates combined with observations of hydrothermal events recorded as discrete layers in sediment cores provide the basis for unravelling the temporal history of the fields. The TAG field shows intermittent activity over the past 120,000 years as evidenced by ages of low-temperature Mn oxides. The presently active black smoker mound first formed about 40,000–50,000 years ago with precipitation of massive sulfides. It has had intermittent, pulsed high-temperature activity every 5000–6000 years over the past 20,000 years which may reflect renewed magmatic activity at the ridge axis. Fluid flow is focussed at the mound site by structural and tectonic control suggested by the intersection of N–S ridge parallel lystric normal faults and an E–W transform fault. Periods of inactivity are marked by covering of the mound with pelagic carbonate ooze which is probably partially dissolved and reprecipitated as aragonite at the end of each high-temperature event. The Snakepit field had an initial event about 4000 years ago, probably shortly after the eruption of the volcanic ridge on which it sits. A recent renewal, still presently active, was probably initiated by recent fissuring of the volcanic pile.

1. Introduction

The hydrothermal phenomena that take place near or at mid-ocean ridges are directly linked to the tectonic and magmatic activity associated with seafloor spreading. They are characterized by different kinds of deposits: hydrothermal sediments, found sporadically along the mid-ocean ridges, which provide a background on which are superimposed episodic flashes represented either by high-temperature (up to 350°C) polymetallic sulfide deposits, or by lower-temperature iron and manganese oxide precipitates. To understand the evolution with time of such episodic systems, we have used radiochronological methods to study the TAG hydrothermal field on the Mid-Atlantic Ridge (MAR) at about 26°N, and the Snakepit field at 23°N (Fig. 1). We use here "high-temperature" events for those forming sulfide chimneys (black or white smokers) and "low-temperature" deposits for those formed after mixing with oxidizing and cold seawater: Mn and Fe oxides.

The TAG hydrothermal field was first discovered in 1972 as part of TAG (Trans Atlantic Geotraverse) project [1]. At that time the field was

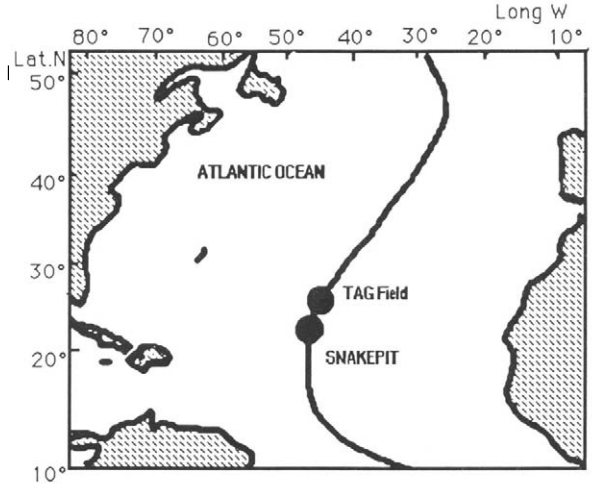

Fig. 1. General map showing the position of TAG and Snakepit hydrothermal fields.

0012-821X/90/$03.50

thought to be characterized only by Ma-oxide deposits of hydrothermal origin [2,3]. These studies are presented by Rona [4] where the hydrothermal characteristics of the field are summarized: heat flow anomalies, magnetic anomalies, large Mn-oxide deposits as evidenced by bottom photography and chemical analyses on dredged samples, punctual temperature anomalies in the bottom waters, variability and excess of ^{3}He associated with the temperature anomalies, excess of Fe and Mn in the suspended particulate matter, and, finally, the presence of metal enrichments in sediment cores. No indications of the possible existence of high-temperature "black smokers" similar to those found on the East Pacific Rise (EPR) were noted, and it was postulated that such phenomenon might be absent at the seafloor surface on slow spreading ridges [4]. New studies in this area in 1982 with the DSRV "Alvin" led to the discovery of an extensive field of low-temperature hydrothermal deposits including manganese oxides, iron oxides and iron silicates [5]. These were described by Thompson et al. [6], and radiochemically dated by Lalou et al. [7]. The occurrence of episodic high-temperature hydrothermal activity was inferred from the presence of discrete Cu-Fe-Zn-rich layers in sediment cores [8]. Based on these observations, Rona et al. [5] postulated that hydrothermal activity was cyclic, with episodic low- and high-temperature stages related to magmatic injection events at a periodicity of about 10^4 years. In August 1985, the first black smokers were photographed in the TAG field, and polymetallic sulfide samples were dredged [9,10]. Three dives with DRSV "Alvin" were undertaken in May 1986 on these black smokers, and water and sulfide samples were recovered [11,12].

In October 1985, ODP Leg 106 found black smokers and massive sulfides (Snakepit hydrothermal field) on the MAR axis at 23°N [13,14]. DSRV "Alvin" dove on the Snakepit in 1986 recovering various samples [11,12]. Further dives with DSRV "Nautile" have also been reported [15].

The main thrust of this paper is to examine the temporal activity of the TAG hydrothermal field as recorded by geochronological analyses of various precipitates. Some preliminary data relevant to temporal activity at Snakepit are also presented.

2. Geochronological methods

Analytical techniques for dating hydrothermal deposits and the conditions and assumptions necessary to apply them have been extensively discussed in Lalou and Brichet [16].

2.1. Sulfide deposits

The $^{210}Pb/Pb$ method may be applied to recent sulfide deposits less than 200 years old. The basic assumption is that the ^{210}Pb and the lead are directly derived from the water–rock interaction, and not scavenged from the overlying seawater; this assumption has been shown to be generally valid [16] and that the ^{210}Pb is not supported by ^{226}Ra. The decrease of ^{210}Pb with its 22 years half-life allows ages determinations back to about 200 years provided the $^{210}Pb/Pb$ ratio at t_0 (time zero) is known. This ratio can be established by measurement of the particulate matter issuing from the active black smokers. The use of this instantaneously measured ratio also assumes that it is constant in all the vents of a given field and remains constant for the life time of the field. This has been partly verified on a field of the EPR at 12°50′N where the same ratio was measured in four different vents along the active area, and on a time scale of 6 years; however, this ratio is not the same as that in other fields of the EPR such as 21°N, 18°S, 20°S or on the MAR (Lalou and Brichet, unpublished data). If a direct measurement of the $^{210}Pb/Pb$ in the particulate matter cannot be done, another possibility is to measure it in the anhydrite associated with the sulfide because anhydrite is not stable under these conditions [17] and soon dissolves so its $^{210}Pb/Pb$ ratio has no time to decrease and is near the t_0 ratio. However, this may result in an underestimate of t_0 because the dissolution is not instantaneous and may actually take several years specially for massive anhydrite deposits. Another possibility, for a specific hydrothermal field, is to consider the highest ratio found to be the initial ratio. In this case the calculated ages are not absolute but relative ages. In certain cases when the youngest samples contain ^{228}Ra, it is possible to cross-check the $^{210}Pb/Pb$ ages by measuring the $^{228}Th/^{228}Ra$ age and thus establish the $^{210}Pb/Pb$ ratio at t_0.

Older samples (between about 500 and 350,000 years old) may be dated by the $^{230}Th/^{234}U$ tech-

nique. This method is based on the fact that in freshly deposited sulfides there is no thorium but some uranium [18]. For these samples care must be taken to avoid oxidized regions because such areas may have incorporated uranium from the surrounding seawater and this makes them appear too young [16].

Thus the $^{210}Pb/Pb$ method allows the study of the detailed history of an active field, and the development of individual chimneys [19], or complex edifices [20], whilst the $^{230}Th/^{234}U$ method gives indications about the periods of activity and quiescence in the past [19,21,22].

2.2. Manganese oxide deposits

Hydrothermal manganese oxide deposits of the FAMOUS area [23], of the Galapagos hydrothermal mounds area [24] and of the Philippine Sea [25] have been dated by $^{230}Th/^{234}U$ technique. Similar deposits from the TAG area have also been dated [3,7]. As with sulfides the assumption is that no thorium isotopes are incorporated at the time of precipitation; the absence of ^{232}Th is used to confirm this hypothesis. Manganese oxide deposits are generally precipitated from low-temperature solutions when the high-temperature solution is cooled and covers the whole spectrum of various hydrothermal precipitates from low to high temperature and thus allows a comprehensive history to be reconstructed.

2.3. Carbonate deposits

In the TAG hydrothermal field calcium carbonate is found as calcite in foraminiferal ooze, and as crystalline aragonite in veins and coatings [11]. These can be dated by the ^{14}C method utilizing linear accelerator mass spectrometry. The ^{14}C ages measured need to be corrected for the reservoir effect (difference between atmosphere and ocean surface plus the difference between ocean surface and deep Atlantic waters, i.e. about 850 years, considering as a first approximation that this aragonite has precipitated directly from the deep sea reservoir). This correction leads to conventional ^{14}C dates.

3. Geologic setting

3.1 TAG hydrothermal field

Hydrothermal activity at the TAG field is located on a 10 km long segment of the eastern wall of the MAR spreading axis [26,27]. At this location the east wall forms a broad salient toward the spreading axis and is made up of a series of fault block steps. High-temperature, presently active black smokers are located at 26°08′N, 44°49′W at the juncture between the rift valley floor and the east wall at 3620–3675 m depth. A zone of low-temperature activity occurs on the east wall between 2400 and 3100 m depth. Sediment cores recovered on the east wall and containing Mn oxide enrichment and discrete layers of sulfides, indicate that much of the region has been the focus of hydrothermal activity at different times in the past. Fig. 2 shows a map of the TAG field with the location of high- and low-temperature deposits (from [10]), and Fig. 3 shows a cross-section of the region at 26° N through the various deposits.

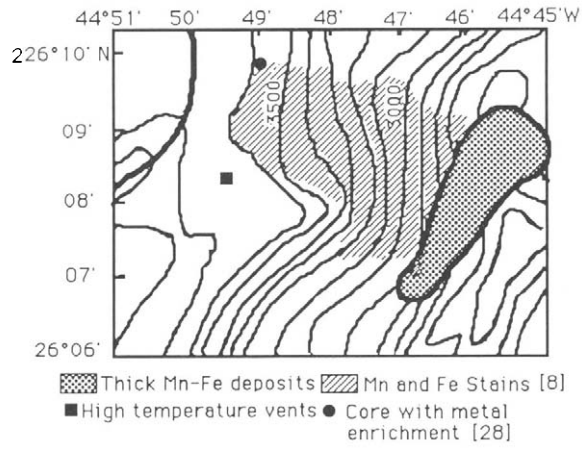

Fig. 2. Bathymetric map (100 m contours) showing the emplacements of the principal mineralizations (modified from Rona [10]).

High-temperature deposits. The presently active high-temperature field lies on oceanic crust about 100,000 years old, as determined from the spreading rate calculated from magnetic anomalies, slightly off the ridge axis [11]. It is made up of an elliptical compound mound consisting of concentric inner and outer portions. The inner mound is about 200 m in diameter and the outer mound is about 500 m wide. The outer mound is covered with carbonate ooze up to a few tens of centimeters in thickness. Basalt talus and occasional massive sulfide blocks outcrop through the ooze at the tops of small ridge structures. The presently active

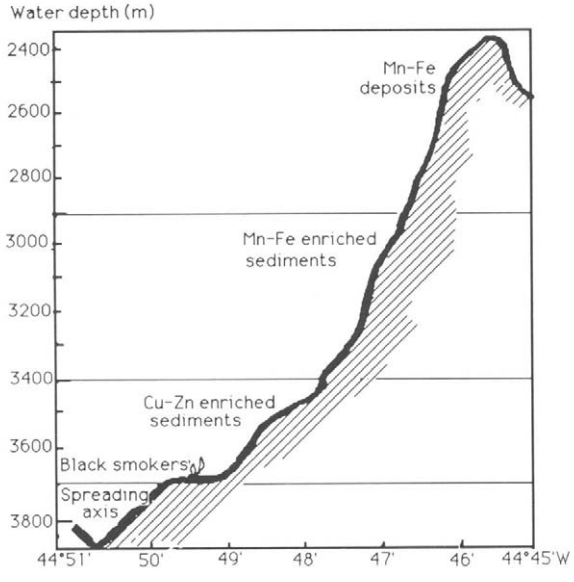

Fig. 3. Schematic cross-section of the eastern wall of the MAR at latitude 26° N. Vertical exaggeration 10:1.

inner mound (Fig. 4) is very steep and rises 50 m above the outer mound [11]. Its outer portion is marked by shimmering water discharging from cracks between massive sulfide talus blocks and relict chimney fragments. At one location on the mound there is a 20 m diameter zone of small 1–2 m high bulbous chimneys emanating white to blue-gray smoke. This region was named the "Kremlin" [11] because of the distinctive, bulbous shape of the chimneys. The central part of the mound is capped by black smoker chimneys rising some 5–10 m high over a region of 30–40 m diameter.

The black smokers are predominantly composed of pyrite, marcasite, and chalcopyrite with small granules of anhydrite. Large massive anhydrite blocks occur near the base of the chimneys. The white smokers of the Kremlin region are predominantly composed of sphalerite, with chalcopyrite, pyrite and anhydrite. The mound itself is mainly composed of massive sulfide blocks and fallen chimneys of chalcopyrite, pyrite and sphalerite. Old vent conduits and fissures in these blocks are commonly coated and infilled with crystalline aragonite. Many of the older blocks have oxidized outer portions and occasional coatings of iron oxide (goethite).

Low-temperature deposits. The metalliferous deposits of the low-temperature field about 1000 m higher on the east wall have been described by Thompson et al. [6]. They include widespread surficial staining of carbonate ooze by Mn oxides, as well as discrete (1 m to 15 × 20 m) massive deposits of manganese oxide (birnessite), amorphous hydrated iron oxide, and iron silicates (nontronite). They include thick laminated crystalline birnessite slabs, small Fe-oxide tubular vents, and loose earthy interlayered birnessite, nontronite and Fe-oxide precipitates. Metal enrichments in subsurface layers in sediment cores are attributed to past episodes of venting [8,28].

3.2. *Snakepit hydrothermal field*

The Snakepit field is located on the MAR at 23° 22.08′N, 44°57.00′W, atop a large volcanic ridge in the axial region [11]. The ridge is 400–600 m high, 40 km in length and is composed of a

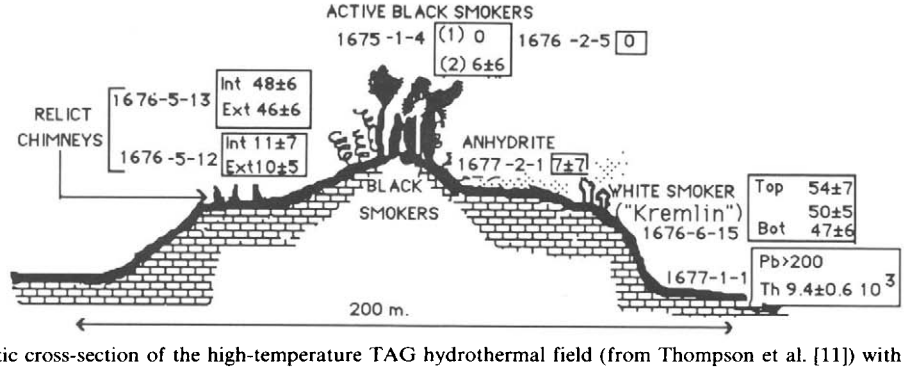

Fig. 4. Schematic cross-section of the high-temperature TAG hydrothermal field (from Thompson et al. [11]) with the positions and ages (in years) of the studied samples. Vertical exaggeration 1:1.

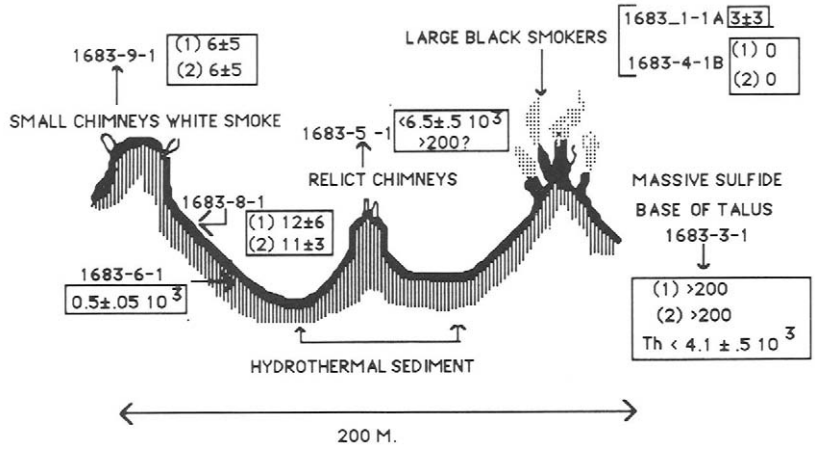

Fig. 5. Schematic cross-section of the Snakepit hydrothermal field (from Thompson et al. [11]) with the positions and ages (in years) of the studied samples. Vertical exaggeration 1 : 1.

series of discrete pillow flows. Volcanic activity ceased some time ago and there is a slight dusting of pelagic ooze. Fissuring of the feature is apparently fairly recent although not yet well developed. The hydrothermal field is at 3400–3480 m water depth on the ridge and covers discontinuously an area 40,000–50,000 m^2 bounded by fissures and faults. The field consists of three elongate, parallel ridges each about 20–30 m high and 100 m long surrounded by sulfide talues and hydrothermal sediment. Each is topped by chimney structures. Fig. 5 shows a cross-section through the field. The easternmost ridge has 10–12 large complex chimneys each about 10 m high and giving off black smoke and has 10–12 large complex chimneys each about 10 m high and giving off black smoke and high-temperature (350 °C) waters [12]. The central ridge has only relict chimneys and is inactive. The westernmost ridge has small bulbous white smokers emanating warm (270 °C) solutions.

The active black smokers are composed principally of pyrite, marcasite, pyrrhotite, chalcopyrite, and anhydrite. The relict chimneys of the central ridge are pyrite and chalcopyrite. The white smokers of the western ridge are predominantly sphalerite, pyrite and marcasite. The Snakepit field differs from the TAG field by the presence of pyrrhotite as a major phase in the Snakepit active high-temperature chimneys. Secondary sulfides and oxidation products are much less abundant than observed at TAG, and aragonite is absent.

4. Results

4.1. TAG field

Recent activity — $^{210}Pb/Pb$ measurements. The results of $^{210}Pb/Pb$ analyses are given in Table 1A, and shown in Fig. 4. Details about the individual samples analyzed are given in Fig. 6A–F. All of the samples, with the exception of one sulfide (Dr 1-1-44) and one piece of anhydrite (Dr 1-1-4) which are dredged material, were recovered by submersible in May 1986 [1].

No black smoker particles were available for analysis, so the $^{210}Pb/Pb$ ratio at t_0 was not directly obtainable. However, analyses of active black smoker chimney walls (two subsamples of 1676-2-5 and subsample (1) of 1675-1-4) give values for the ratio that are equal within statistical errors, and their mean value of 1.39 ± 0.14 is taken as the initial ratio. In all sampling care was taken to avoid any oxidized part which could induce erroneous results. All of the ^{210}Pb values have been corrected for the time elapsed between the date of measurement and the date of sampling. γ-ray measurements did not show significant activity of ^{226}Ra relative to ^{210}Pb activity, so that the total ^{210}Pb represents excess ^{210}Pb.

The ages of the most recent chimneys are 0–50 years.

Relict chimneys — $^{230}Th/^{234}U$ measurements. The $^{230}Th/^{234}U$ analyses of older samples are given in

Table 1B. Details about the individual samples are given in Fig. 6G–P. Aragonite samples dated by ^{14}C are also given in Table 1B. All of the samples are from a dredge haul made in 1985, with the exception of one submersible sample (1677-1-1) recovered from the outer edge of the inner mound. The dredge haul covered part of the outer mound and onto the outer edge of the inner mound [10].

The ages of the relict chimneys vary between 5000 and 30,000 years.

Low-temperature deposits — $^{230}Th/^{234}U$ measurements. These results have been reported previously [7]. They were done predominantly on layered Mn-oxide samples. Most of the ages range between 4000 and 16,000 years with the most active periods around $15{,}000 \pm 1000$ and 7000 ± 3000 years. Some older samples were also measured and gave ages of 30, 47, 100 and 125×10^3 years.

4.2. Snakepit field

This study has been limited to the few samples recovered by Alvin dive 1683 [11,12] because the ODP drilled samples [13,14] were too fragmented to be representative and the samples from Nautile dives [15] were not yet available. $^{210}Pb/Pb$ measurements of recently or presently active chimneys are given in Table 2A. $^{210}Pb/Pb$ ratio at t_0 has been taken as the highest ratio found in the field (1.17 ± 0.09) for sample 1683-4-1-B, slightly lower than in TAG field, but the difference between the two corresponds only to a 5-year discrepancy.

TABLE 1A

$^{210}Pb/Pb$ results for TAG youngest samples

Sample No.	Mineralogy [a]	^{210}Pb (dpm g^{-1})	Pb (ppm)	$^{210}Pb/Pb$	Age (years)
1676-2-5					
(1)	C, P, M	177 ± 11	130 ± 6	1.36 ± 0.11	0
(2)	C	40.6 ± 2.4	28 ± 2.8	1.45 ± 0.17	0
1675-1-4					
(1)	C, A	10.0 ± 0.5	7.3 ± 0.7	1.37 ± 0.15	0
(2)	A, G	20.0 ± 0.9	17.3 ± 1.7	1.16 ± 0.13	6 ± 6
1677-2-1					
	A	0.32 ± 0.03	0.28 ± 0.03	1.14 ± 0.16	7 ± 7
1676-5-12					
(1)	C, P	66.5 ± 4.1	68 ± 7	0.98 ± 0.11	11 ± 7
(2)	C, S, P	120 ± 7	120 ± 6	1.00 ± 0.08	10 ± 5
1676-5-13					
(1)	S, Zn, C	64.3 ± 3.9	210 ± 10	0.31 ± 0.02	48 ± 6
(2)	S, Zn	184 ± 9	570 ± 28	0.32 ± 0.02	46 ± 6
1676-6-15					
Top					
(1)	C, S	15.4 ± 1.2	62 ± 6	0.25 ± 0.03	54 ± 7
(2)	S, Zn	115 ± 7	392 ± 20	0.29 ± 0.02	50 ± 5
Base					
(1)	S, Zn	125 ± 8	387 ± 19	0.32 ± 0.02	47 ± 6
1677-1-1					
(1)	P, M	0.83 ± 0.07	342 ± 17	0.0024 ± 0.0002	> 200
(2)	P, M	0.747 ± 0.045	330 ± 16	0.0023 ± 0.0002	> 200
(3)	P, M	0.337 ± 0.041	400 ± 20	0.0008 ± 0.0001	> 200
1676-1-1					
	S, Zn	205 ± 10	618 ± 30	0.33 ± 0.02	46 ± 5
Dr1-1-44					
	A	62.4 ± 3.2	53.5 ± 2.7	1.17 ± 0.08	5 ± 5
Dr1-1-4					
	A	1.29 ± 0.09	1.43 ± 0.14	0.9 ± 0.10	14 ± 7

Errors quoted are 1σ counting error for ^{210}Pb and 5% or 10% for lead depending on the concentration and then of the method used.

[a] Mineralogy: C = chalcopyrite; P = pyrite; M = marcasite; S = sphalerite; A = anhydrite; G = gypsum; Zn = hydrated zinc sulfate; Fe = iron oxide. Minerals are quoted in order of decreasing abundance in the subsamples.

TABLE 1B

$^{230}Th/^{234}U$ and ^{14}C dating for samples dredged on TAG hydrothermal field

Sample No.	$^{234}U/^{238}U$	^{234}U (dpm g^{-1})	^{230}Th (dpm g^{-1})	^{232}Th (ppm)	$^{230}Th/^{234}U$	Age ($\times 10^3$ years)
1677-1-1	1.143 ± 0.017	9.31 ± 0.22	0.78 ± 0.04	n.d.	0.083 ± 0.003	9.4 ± 0.6
Dr1-23						
Aragonite (3)	1.126 ± 0.043	3.53 ± 0.13	0.18 ± 0.01	n.d.	0.051 ± 0.004	5.7 ± 0.6
Aragonite + nontronite (2)	1.095 ± 0.037	4.49 ± 0.15	0.22 ± 0.002	n.d.	0.049 ± 0.004	5.5 ± 0.5
Sulfide + 33% aragonite (1)	1.167 ± 0.051	2.51 ± 0.11	0.27 ± 0.002	n.d.	0.108 ± 0.008	12.4 ± 1
Aragonite conventional ^{14}C [a] Gif	–	–	–	–	–	3.88 ± 0.12
Real ^{14}C age estimate [b]						4.3
Sulfide calculated from (1) and ^{14}C aragonite [c]	–	–	–	–	–	19
Dr1-1-8						
67% Aragonite + goethite (1)	1.093 ± 0.060	3.38 ± 0.14	0.34 ± 0.05	0.36 ± 0.1	0.099 ± 0.014	11.3 ± 1.7
52% Aragonite + sulfide (2)	1.108 ± 0.033	2.34 ± 0.07	0.32 ± 0.03	n.d.	0.136 ± 0.012	15.8 ± 1.5
Sulfide (4)	1.264 ± 0.081	1.53 ± 0.11	0.29 ± 0.01	n.d.	0.189 ± 0.016	22.5 ± 2
Aragonite conventional ^{14}C [a] Gif	–	–	–	–	–	8.52 ± 0.12
Real ^{14}C estimate [b]						9.5 *
Goethite calculated from (1) and ^{14}C aragonite [c]	–	–	–	–	–	17
Sulfide calculated from (2) and ^{14}C aragonite [c]	–	–	–	–	–	40
Dr1-1-46						
Aragonite (5)	1.152 ± 0.055	3.69 ± 0.02	0.237 ± 0.028	n.d.	0.064 ± 0.008	7.2 ± 1
Goethite + 14% aragonite (3)	1.048 ± 0.078	4.48 ± 0.32	1.059 ± 0.054	n.d.	0.236 ± 0.021	29.0 ± 3
Sulfide (1)	1.099 ± 0.013	3.74 ± 0.10	0.474 ± 0.026	n.d.	0.127 ± 0.008	14.7 ± 1
Aragonite conventional ^{14}C [a] Gif	–	–	–	–	–	3.31 ± 0.09
Real ^{14}C estimate [b]						3.6
Goethite calculated from (3) and ^{14}C aragonite [c]	–	–	–	–	–	32.5
Dr1-1-21						
Aragonite + sulfides (2)	1.191 ± 0.044	5.02 ± 0.23	0.662 ± 0.048	n.d.	0.132 ± 0.011	15.3 ± 1.4
Sulfide + 10% aragonite (1)	1.141 ± 0.087	1.31 ± 0.08	0.279 ± 0.088	n.d.	0.213 ± 0.025	26.0 ± 3.5
Aragonite conventional ^{14}C [a] Gif (A)	–	–	–	–	–	2.94 ± 0.1
Real ^{14}C estimate [b]						3.2
Aragonite conventional ^{14}C [a] Gif (B)	–	–	–	–	–	3.52 ± 0.09
Real ^{14}C estimate [b]						3.9
Aragonite conventional ^{14}C [a] Gif (C)	–	–	–	–		8.49 ± 0.14
Real ^{14}C estimate [b]						9.5 *
Aragonite conventional ^{14}C [a] Arizona (D)	–	–	–	–	–	6.83 ± 0.07
Real ^{14}C estimate [b]						7.7
Dr1-1-24						
Aragonite (1)	1.194 ± 0.041	5.19 ± 0.18	0.502 ± 0.037	n.d.	0.087 ± 0.008	11.0 ± 1
Sulfide (2)	1.091 ± 0.065	0.77 ± 0.04	0.312 ± 0.029	0.29 ± 0.05	0.404 ± 0.04	56?
Aragonite conventional ^{14}C [a] Arizona (A)	–	–	–	–	–	5.80 ± 0.07
Real ^{14}C estimate [b]						6.55
Aragonite conventional ^{14}C [a] Gif (B)	–	–	–	–	–	6.99 ± 0.49
Real ^{14}C estimate [b]						7.8
Dr1-1-43						
Aragonite (1)	1.085 ± 0.041	4.07 ± 0.19	0.321 ± 0.026	n.d.	0.079 ± 0.007	8.9 ± 0.8
Sulfide (2)	1.356 ± 0.165	0.43 ± 0.04	0.081 ± 0.01	n.d.	0.186 ± 0.029	22 ± 4
Carbonate ooze conventional ^{14}C [a] Arizona						7.61 ± 0.06
Real ^{14}C estimate [b]						8.4

TABLE 1B (continued)

Sample No.	$^{234}U/^{238}U$	^{234}U (dpm g^{-1})	^{230}Th (dpm g^{-1})	^{232}Th (ppm)	$^{230}Th/^{234}U$	Age ($\times 10^3$ years)
Dr1-1-45						
Sulfide (1)	1.139 ± 0.045	0.32 ± 0.01	0.012 ± 0.001	n.d.	0.037 ± 0.003	4.0 ± 0.5
Sulfide (2)	1.074 ± 0.044	0.46 ± 0.02	0.019 ± 0.004	0.01 ± 0.01	0.041 ± 0.009	4.5 ± 1
DR1-1-16						
Sulfide (1)	1.166 ± 0.036	1.94 ± 0.12	0.243 ± 0.02	n.d.	0.125 ± 0.012	14.4 ± 1.5
Aragonite (2)	1.162 ± 0.029	4.19 ± 0.15	0.667 ± 0.071	n.d.	0.159 ± 0.018	18.7 ± 2.3
Aragonite conventional ^{14}C [a] Gif (A) richer in sulfide	–	–	–	–	–	3.92 ± 0.1
Real ^{14}C estimate [b]						4.5
Aragonite conventional ^{14}C [a] Gif (B) richer in goethite	–	–	–	–	–	5.76 ± 0.1
Real ^{14}C estimate [b]						6.5
Dr1-1-7D						
Loose internal sulfide (1)	1.178 ± 0.034	18.81 ± 1.2	1.899 ± 0.095	n.d.	0.101 ± 0.08	11.5 ± 1
External goethite (2)	1.132 ± 0.041	13.62 ± 0.83	1.722 ± 0.155	n.d.	0.126 ± 0.014	14.6 ± 1.8
Central sulfide (3)	1.217 ± 0.019	12.36 ± 0.62	1.752 ± 0.137	n.d.	0.142 ± 0.013	16.5 ± 1.7
Dr1-1-15						
Aragonite (1)	1.079 ± 0.055	7.71 ± 0.47	2.105 ± 0.211	n.d.	0.273 ± 0.032	34.5 ± 5
Sulfide (2)	1.096 ± 0.013	94.43 ± 5.18	14.68 ± 0.84	n.d.	0.155 ± 0.012	18.3 ± 1.5
Goethite (3)	1.026 ± 0.073	2.98 ± 0.22	0.906 ± 0.095	n.d.	0.292 ± 0.034	37.7 ± 5.3
Sulfide (4)	1.164 ± 0.121	5.38 ± 0.43	0.898 ± 0.191	n.d.	0.167 ± 0.038	20 ± 5
Aragonite (5)	1.092 ± 0.183	5.78 ± 0.73	2.05 ± 0.46	n.d.	0.355 ± 0.04	47 ± 17
Aragonite conventional ^{14}C [a] Gif	–	–	–	–	–	3.62 ± 0.1
Real ^{14}C estimate [b]						4
Dr1-1-3						
Iron oxide (1)	1.134 ± 0.052	3.17 ± 0.15	0.934 ± 0.064	0.08 ± 0.03	0.295 ± 0.025	37.5 ± 4
Dr1-1-44						
Sulfide	1.009 ± 0.035	2.65 ± 0.15	n.d.	n.d.	n.d.	n.d.
Sulfide (^{210}Pb)						(see Table 1A)

[a] Conventional ^{14}C is the measured value corrected for the difference between atmosphere and deep Atlantic Waters, ca. −850 years [43] assumed to be constant during the last 10,000 years. (If the origin of carbonate is sediment formed with planktonic species, the correction is only −400 years.)

[b] Real age estimate. In order to compare these ages with ages obtained by other radiochronological methods, we have used the ^{14}C calibration curves for the atmosphere measured in tree rings [44]. * Around 9000 B.P., the $\Delta^{14}C$ of the atmosphere is close to 90‰ [45]. These estimates are probably affected by an uncertainty of about ±300 years, due to uncertainties of the real reservoir age correction and to the response of the deep ocean to the ^{14}C atmosphere variations.

[c] Calculated ages = age of the mixture sulfide (or goethite) + aragonite corrected for the % aragonite in the sample and the ^{14}C age of aragonite.

n.d. = non detected, i.e. under the detection limit taken as $\sqrt{2N}$, N being the averaged number of counts at the ^{232}Th energy area. It is fluctuant, owing to the quantity of sample available and the counting time.

Quoted errors are 1σ counting error.

Older samples analyzed by the $^{230}Th/^{234}U$ method are given in Table 2B. A description of individual samples is given in Fig. 7. The youngest samples are 0–12 years old, the oldest are between 500 and perhaps 5000 years.

5. Discussion

In Fig. 8 we have summarized all the available data for ages of different deposits in the TAG hydrothermal field; the chronology of Snakepit is not sufficiently well established to be included in the figure, and specially because we cannot ascertain that the two fields followed the same temporal evolution. Column 1 shows our measurements on relatively pure sulfides. Column 2 shows data from sediment cores in the TAG field in which discrete layers of sulfide or Cu-Fe-Zn enrichment have been reported [8,28]. These and many other cores also show sulfide or metal staining at the seawater–sediment interface, presumably of present-day age (0–100 years). The ages of

the enriched layers were calculated in the cores from their depth assuming a constant sedimentation rate of 1.8 cm ky^{-1} [8], or in one core from ^{14}C measurements and carbonate accumulation rates (0.6 g cm^{-2} ky^{-1}) which gave ages of two recorded hydrothermal layers as 6000 and 8500 years [28]. Column 3 presents the ages of the aragonite deposits determined by ^{14}C radiochronology. Column 4 shows our previous $^{230}Th/^{234}U$ measurements on manganese deposits from the low-temperature field located at shallower depth (2400–2900 m depth) on the eastern wall [7]. Column 5 shows data on discrete Mn enrichment observed in various cores by other workers [8,28]. Column 6 presents our new measurements on iron oxides.

Two important observations can be made immediately from Fig. 8. First, the hydrothermal activity in the TAG field has been intermittent, or pulsed, over the past 120,000 years. Second, the present activity is relatively recent (< 100 years) after a hiatus of about 4000 years. We recognize that the establishment of a precise chronology depends on a thorough and representative sampling which is difficult to assert in the deep sea environment. However, we note that in studies of the EPR at 21° N, 13° N and in the Galapagos Rift [19,21,22], only very young (< 200 years) were found at active sites, and fossil samples (except for an active low-temperature site at 13° N dated at 2000 years) were about 4000 years or older, in agreement with our findings in the TAG field.

In detail we can note further features of the intermittent activity. Considering the sulfide ages (Fig. 8, column 1) they can be grouped into six

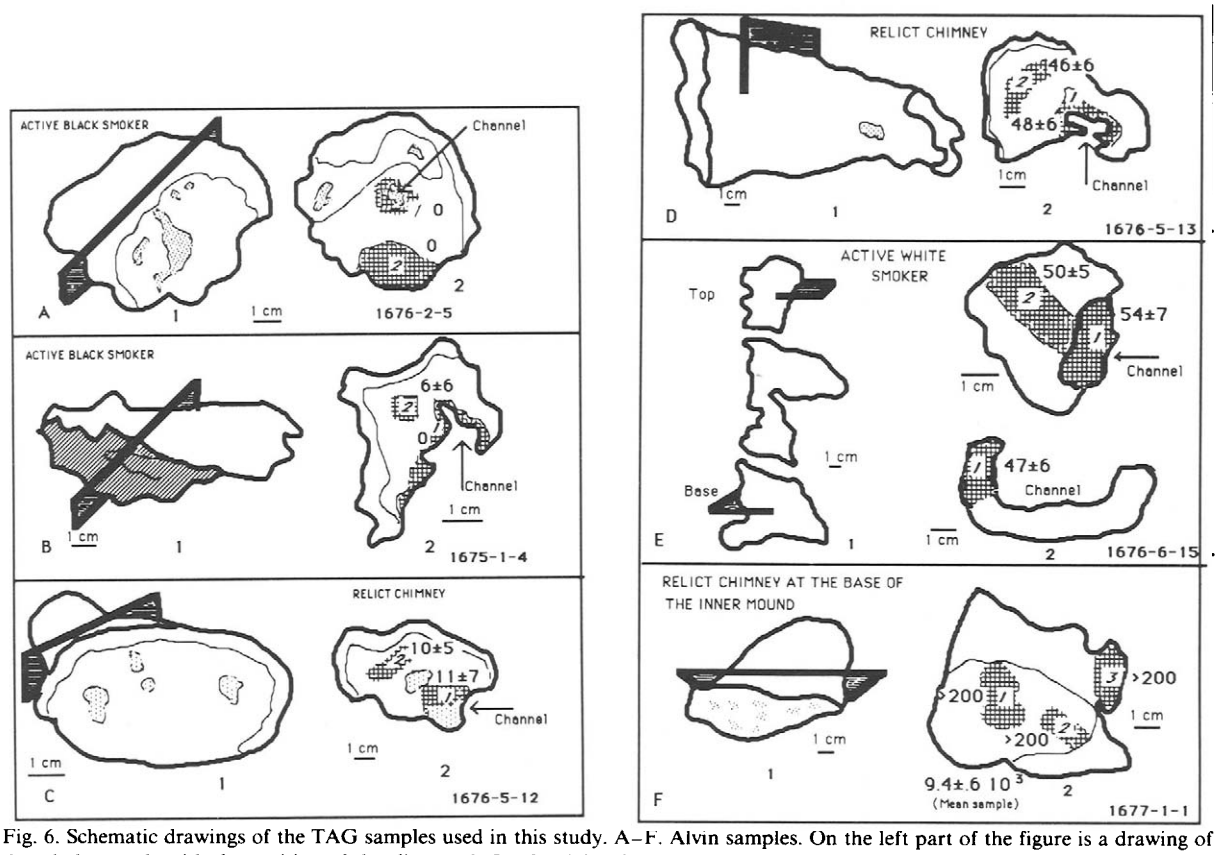

Fig. 6. Schematic drawings of the TAG samples used in this study. A–F. Alvin samples. On the left part of the figure is a drawing of the whole sample with the position of the slice used. On the right, the cross-section of the slice with the position (window bars area and italic numbers) and ages in years (bold numbers) of the subsamples. Feeding channels are indicated by dotted area. G–P. Samples from the 1985 dredge haul. The samples are presented with the different orientations showing the places where the subsamples have been cut. The ages indicated are in ky (bold numbers). The identification of subsample is in italic (numbers for the samples dated with $^{230}Th/^{234}U$, letters followed by ^{14}C for the ones measured with AMS).

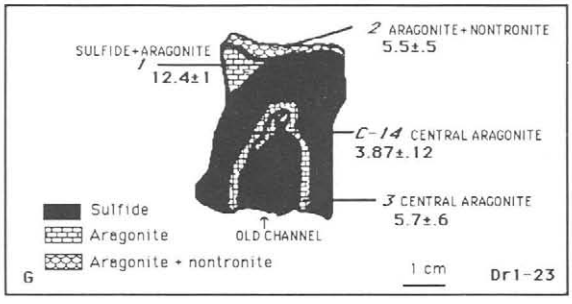

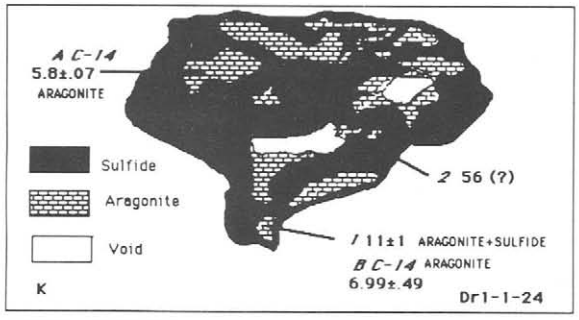

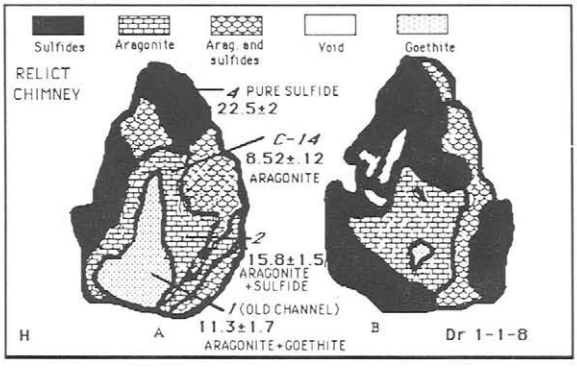

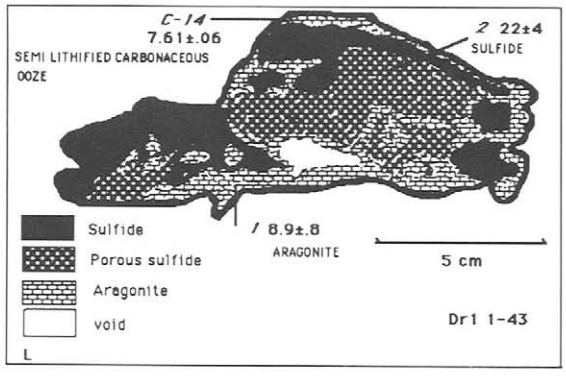

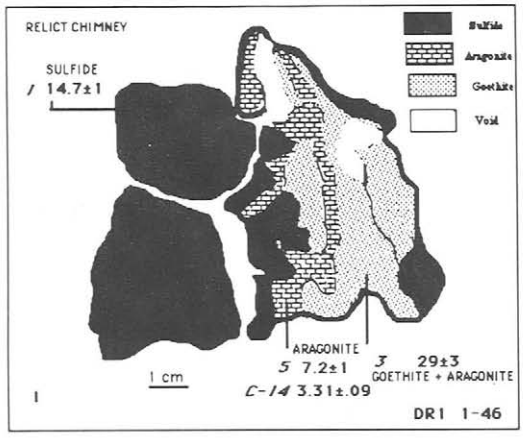

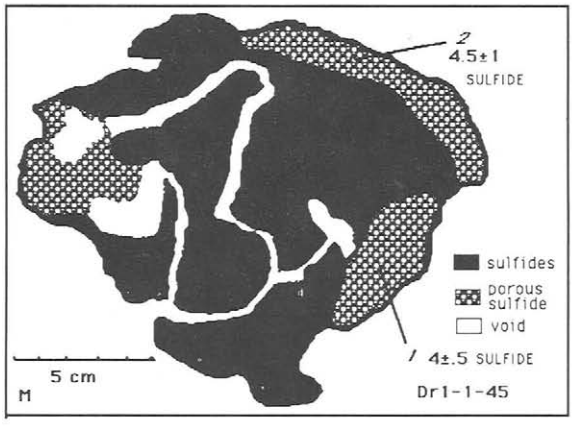

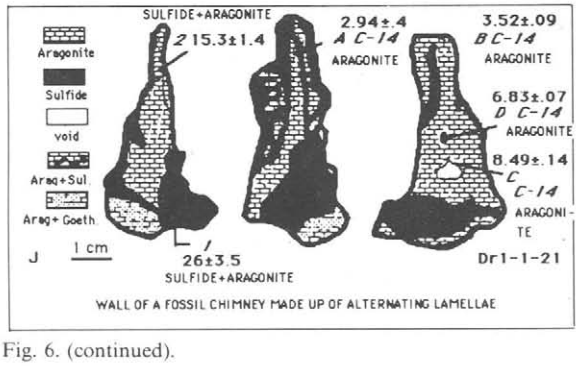

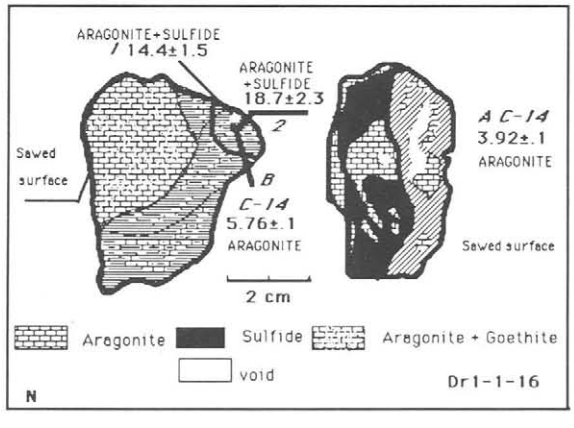

Fig. 6. (continued).

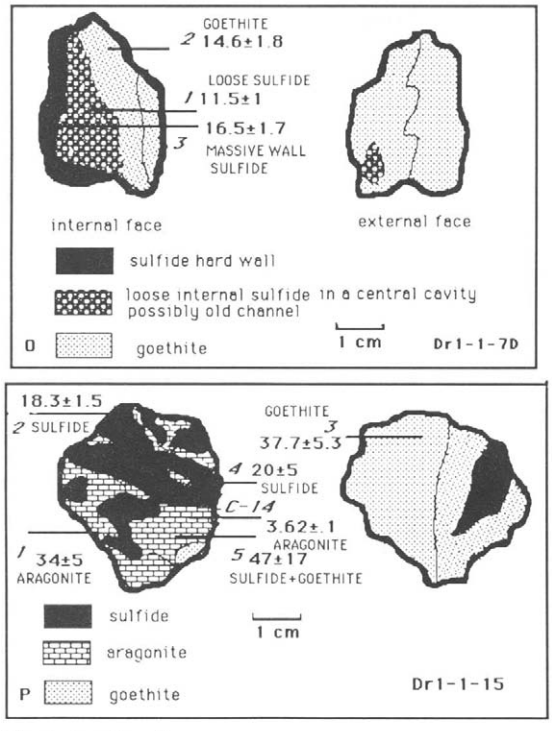

Fig. 6. (continued).

periods. The oldest one is around 50,000 years (2 samples, $40-56 \times 10^3$ years with some large uncertainties), another younger one is around 20,000 years (5 samples, $18.3-26 \times 10^3$ years), then about 15,000 years (3 samples, $14.4-16.5 \times 10^3$ years), 10,000 years (2 samples, $9.4-11.5 \times 10^3$ years) and 4000 years ago (2 samples, $4.0-4.5 \times 10^3$ years). The white smokers and recently inactive chimneys are about 50 years old, including one sample recovered just outside the active inner mound which indicates there has been little recent activity in parts of the outer mound. Present activity includes the black smokers and massive anhydrite which are around 10 years old or less. Between these periods of high-temperature activity leading to the formation of sulfide deposits, there are major gaps in activity, as far as sulfides are concerned.

The data from the cores indicate a number of past events between 4000 and 18,000 years based on sulfide or Mn-rich layers determination. The analyses of the Mn deposits in the low-temperature field indicate past intermittent activity between 4000 and 120,000 years with major events around 7000 and 15,000 years ago. There are only a few analyses of iron oxides and they show ages between 15,000 and 40,000 years ago.

The aragonite precipitations are always younger than their associated sulfides and must represent a different event. They are only found on the high temperature mound, and not observed in nearby

TABLE 2A

$^{210}Pb/Pb$ results for Snakepit youngest samples

Sample No.	Mineralogy [a]	^{210}Pb (dpm g^{-1})	Pb (ppm)	$^{210}Pb/Pb$	Age (years)
1683-4-1B					
(1)	S, Fe	559 ± 41	462 ± 23	1.21 ± 0.11	0
(2)	S, Fe	384 ± 24	327 ± 16	1.17 ± 0.09	0
1683-1-1A					
(1)	Fe	31.5 ± 1.7	29 ± 3	1.09 ± 0.13	3 ± 3
1683-9-1					
(1)	P, M, C	268 ± 14	280 ± 14	0.96 ± 0.07	6 ± 5
(2)	P, M, C	251 ± 12	260 ± 13	0.96 ± 0.07	6 ± 5
1683-3-1					
(1)	P	0.126 ± 0.028	99 ± 5	0.0013 ± 0.0003	> 200
(2)	P	0.045 ± 0.015	294 ± 15	0.00015 ± 0.00005	> 200
1683-8-1					
(1)	S, M	304 ± 21	380 ± 19	0.80 ± 0.07	12 ± 3
(2)	S, M	1541 ± 105	1857 ± 93	0.83 ± 0.07	11 ± 3
1683-5-1					
	P, M, C	0.196 ± 0.020	1444 ± 72	0.00014 ± 0.00002	> 200

Errors quoted are 1σ counting error for ^{210}Pb and 5% or 10% for lead depending of the concentration and then of the method used.
[a] Mineralogy: C = chalcopyrite; P = pyrite; M = marcasite; S = sphalerite; Fe = iron oxide. Minerals are quoted in order of decreasing abundance in the subsamples.

TABLE 2B

$^{230}Th/^{234}U$ dating for samples older than 200 years for Snakepit hydrothermal field

Sample No.	$^{234}U/^{238}U$	^{234}U (dpm g^{-1})	^{230}Th (dpm g^{-1})	^{232}Th (ppm)	$^{230}Th/^{234}U$	Age ($\times 10^3$ years)
1683-3-1 (3)	1.065 ± 0.029	0.253 ± 0.009	0.009 ± 0.001	0.006 ± 0.001	0.037 ± 0.004	< 4
1683-6-1 (1)	1.146 ± 0.028	4.0 ± 0.2	0.016 ± 0.002	n.d.	0.0041 ± 0.0006	0.45 ± 0.07
1683-5-1	1.117 ± 0.044	0.208 ± 0.010	0.012 ± 0.001	0.003 ± 0.001	0.058 ± 0.005	< 6

Errors are statistical counting errors at 1σ level.
n.d. = not detected, i.e. under the detection limit.

cores. Aragonite is not a common constituent of the deep sea environment, although it has been reported in association with deep sea peridotites [29], with hydrothermal sediments in DSDP cores [30] and in the Red Sea Brines [31]. Generally aragonite is unstable in the deep sea environment and will dissolve or invert to calcite; presumably the massive crystalline nature and high Sr content (1.5–2%) helps its preservation [32,33].

The aragonite ages determined by ^{14}C radiochronology fall in three groups: one around 4,000 years (6 samples, 3200–4500 years), a second around 7000 years (4 samples, 6500–7800 years) and a third group around 9000 years (3 samples, 8400–9300 years). Perhaps older aragonite deposits have not been sampled or have been already dissolved. The questions we need to answer are: what is the origin of the aragonite and what do the ages tell us regarding hydrothermal activity?

Swart (personal communication) has shown for one of the aragonite samples (1-23), that $\delta^{18}O$ values lie between +4 and +4.4‰ (vs. PDB) and $\delta^{13}C$ values are between +2.5 and +3.7‰. Following data of Tarutani et al. [34] and Grossman

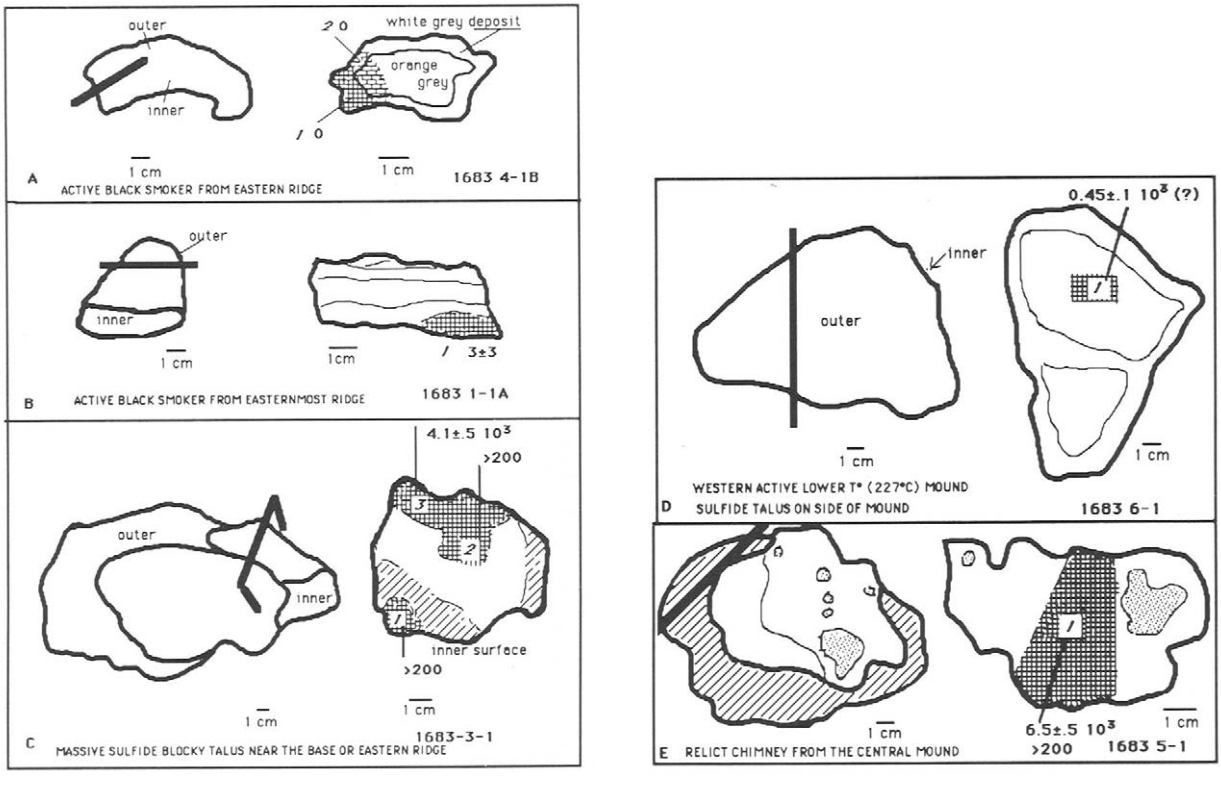

Fig. 7. Schematic drawing of the Snakepit samples. For explanation see caption for Fig. 6A–F.

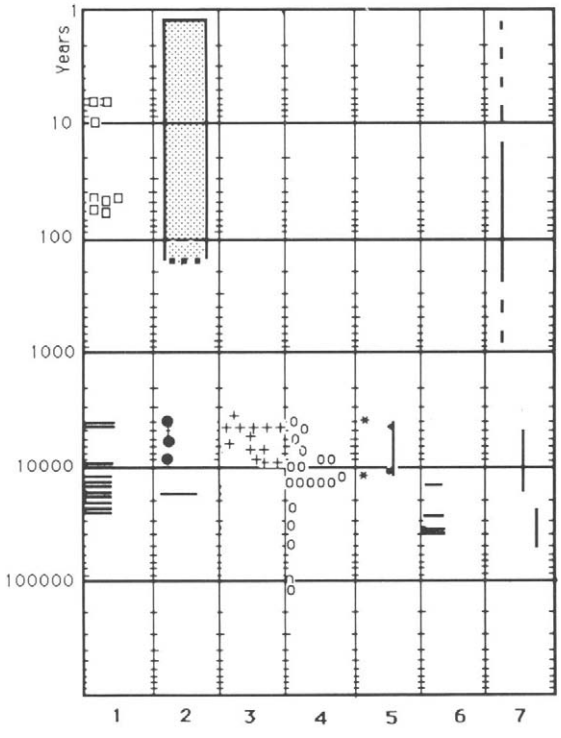

Fig. 8. Summary of the results obtained for the TAG hydrothermal field. The results of age dating for TAG samples are reported on a logarithmic time scale. Column 1 = sulfide samples; 2 = hydrothermal sulfides in cores after Shearme et al. [8] and Metz et al. [28]; 3 = ^{14}C ages of aragonite; 4 = ages of Mn-oxide deposits (from Lalou et al. [7]); 5 = Mn enrichments in cores from Shearme et al. [8] (bar with two peaks) and from Metz et al. [28] (asterisks); 6 = goethite or iron oxide; 7 = eruptive volcanic events (from Zonenshain et al. [39]).

and Ku [35] for determining the temperature of precipitation of aragonite from seawater, this would indicate precipitation at 2.5 ± 1°C, i.e. bottom water temperature for the TAG area. Similar values for $\delta^{18}O$ (+1.4 to +4.4‰) and $\delta^{13}C$ (+2.3 to +4.4‰) were noted for carbonate veins in basaltic rocks at DSDP site 395, 140 km west of the MAR at 23°N [36]. The low-temperature precipitation of aragonite occurred in the voids of the chimneys and not during high-temperature sulfide precipitation. We suggest that the aragonite results from dissolution and reprecipitation of the calcareous ooze settling on the mound when the system cools at the end of an episode of hydrothermal activity. This hypothesis also took into account the fact that we have no very young aragonite associated with the present activity.

The ^{14}C age of the precipitating aragonite depends on the range of age of the reworked sediment; moreover, this ooze being essentially planktonic foraminifera, the reservoir correction for ^{14}C dates will be then limited to the difference between atmosphere and surface waters, that is about −400 years. This range of age of the reworked sediment would explain the range in values within the different age groups of aragonite (about 1000 years), but larger age differences among the groups probably represent discrete periods of hydrothermal activity.

Previous works [6,11,37] suggested that the large salient of the eastern wall, which is made up of a series of lystric fault steps, may affect the plumbing system of the hydrothermal circulation and channel the hydrothermal solutions along major normal faults to their present venting site. Recent work [38] further suggests that a major east–west fault zone is present in the TAG area and is perpendicular to the north–south axis parallel normal fault regime. The TAG mound apparently lies on the intersection of these two faults whose geometry favors focussing of the hydrothermal solutions. They are presumably reactivated at or shortly after each magmatic event. This hypothesis is supported by observations with the two Soviet MIR submersibles in Spring 1988 where they distinguished at least three age groups of lava flows based on sediment cover: old flows of 25,000–50,000 years old; intermediate flows of about 5000–15,000 years old; and young flows less than 1000 years old [39]. Thus the mound provides a historic record of past volcanic, tectonic and hydrothermal events.

The TAG field, because of the ridge topography, differs from hydrothermal fields on the East Pacific Rise where the present and fossil activity are separated in space and time [19,21], and the plume influence may spread well away from the ridge axis to the abyssal plain [40]. The Galapagos mounds formation is similar to the TAG area in showing hydrothermal activity at the same location despite a large shifting (20–30 km) away from the spreading centre over a long time span (600,000 years), based on data from Lalou et al. [41], although in this case it has all been low-temperature deposits (MnO_2, nontronite and no sulfides). The TAG field has high- and low-temperature deposits (sulfides and MnO_2) in close proximity. Low-tem-

perature fluids that reach high on the east wall, about 1000 m higher than the sulfide deposit, are probably related to the major circulation and represent fluids that, mixing with cold seawater, have lost their sulfides within the crust and now only precipitate Fe, Mn and Si. Some of the high-temperature plume activity impacts on the surrounding sediment leading to metal-rich horizons in the sediment column.

The chronology for the Snakepit field is more uncertain because only a few samples have been analyzed. Presently active chimneys, or those recently active, are up to 12 years old. Older samples have some uncertainties because of ^{232}Th contamination but suggest past activity around 4000–5000 years ago. This would be in keeping with an initial hydrothermal activity shortly after eruption of the volcanic ridge. Slight sediment cover on the ridge implies an age of only a few thousand years [42]. This event may have built the large talus ridges and the deep sediment layers (up to 11 m) as reported by the ODP drilling [13,14]. Recent reactivation may have occurred at the onset of fissuring which reopened fluid channelways, or possibly there has been recent reinjection of magma into the magma chamber and reinitiation of hydrothermal circulation. Reactivation and opening of old channelways would also explain the anomalous Cs/Rb and B isotope ratios observed in Snakepit fluids which were ascribed to contact of the present-day fluids with weathered basalts [12].

6. Conclusion

Based on the present sampling and geochronology, we suggest the following history: activity at the TAG hydrothermal field began 120,000 years ago as evidenced by low-temperature hydrothermal activity, and was probably intermittent until about $40–50 \times 10^3$ years ago. At that time the presently active mound began to form. Older high temperature activity has not yet been observed. Intermittent high temperature activity continued with at least four more past high temperature events (20,15,10 and 4×10^3 years ago). The dates obtained on the sulfides from the mound suggest a hiatus from between 10,000 and 4000 years, but dating of layers in the adjacent sediments, and an event that precipitated aragonite, suggest some activity in the region between 6000 and 8000 years ago. Present activity began 50 to 100 years ago.

Repeated events at the same location (the presently active mound) are due to focussing of the vent fluids via major fault systems. The heat source and hydrothermal circulation are driven by magmatic injection at or near the ridge axis. Age data from the sulfides suggest, at least for the past 20,000 years, that new hydrothermal circulation (and hence magma injection) occurs every 5000–6000 years.

The Snakepit field appears to have registered at least two events, an initial event about 4000 years ago, and a recent revival which is still presently active. As with the TAG hydrothermal field, the hydrothermal activity is apparently tectonically controlled, although driven by magmatic events, but these first results have to be confirmed on new well documented samples.

Acknowledgements

We thank S. Humphris and M. Sulanowska for help in the laboratory and the mineralogical work on the sulfides; L. Toolin and A.J. Jull for the Arizona AMS results, and S. Griffin and A. Witter for sample preparation; E. Kaltnecker and P. Maurice for the preparation of samples for the French AMS Carbon-14 dating, D. de Zertucha, A. Castera and J. Dudouit for technical assistance in keeping the Tandetron operating. Funding was provided for the French part from CNRS and CEA and from grant 5141 from PNEHO, and for the U.S. part from NSF grants 87-12136 and the Mellon Foundation. This is Woods Hole Contribution No. 7093 and CFR Contribution 1044.

References

1 P.A. Rona, Marine Geology, in: McGraw-Hill Year Book of Science and Technology, pp. 252–256, McGraw-Hill, New York, N.Y., 1973.
2 R.B. Scott, P.A. Rona, B.A. McGregor and M.R. Scott, The TAG hydrothermal field, Nature 251, 301–302, 1974.
3 M.R. Scott, R.B. Scott, P.A. Rona, L.W. Butler and A.J. Nalwalk, Rapidly accumulating manganese deposit from the median valley of the Mid-Atlantic Ridge, Geophys. Res. Lett. 1, 335–358, 1974.
4 P.A. Rona, TAG hydrothermal field: Mid-Atlantic Ridge crest at latitude 26°N, J. Geol. Soc. London 137(4), 385–402, 1980.

5 P.A. Rona, G. Thompson, M.J. Mottl, J.A. Karson, W.J. Jenkins, D. Graham, M. Mallette, K. Von Damm and J.M. Edmond, Hydrothermal activity at the Trans Atlantic Geotraverse hydrothermal field, Mid-Atlantic Ridge crest at 26° N, J. Geophys. Res. 89(B13), 11365–11377, 1984.
6 G. Thompson, M.J. Mottl and P.A. Rona, Morphology, mineralogy and chemistry of hydrothermal deposits from the TAG area, 26° N, Mid-Atlantic Ridge, Chem. Geol. 49, 243–257, 1985.
7 C. Lalou, G. Thompson, P.A. Rona, E. Brichet and C. Jehanno, Chronology of selected hydrothermal deposits from the Trans Atlantic Geotraverse "TAG" area, Mid-Atlantic Ridge, 26° N. Geochim. Cosmochim. Acta 50, 1737–1743, 1986.
8 S. Shearme, D.S. Cronan and P.A. Rona, Geochemistry of sediments from the TAG hydrothermal field, Mid Atlantic Ridge at latitude 26° N, Mar. Geol. 51, 269–291, 1983.
9 P.A. Rona, Black smokers and massive sulfides at the TAG hydrothermal field, Mid-Atlantic Ridge 26° N, EOS 46, 936, 1985 (abstract).
10 P.A. Rona, G. Klinkhammer, J.A. Nelsen, J.H. Trefry and H. Elderfield, Black smokers, massive sulphides and vent biota at the Mid-Atlantic Ridge, Nature 321, 33–37, 1986.
11 G. Thompson, S.E. Humphris, B. Schroeder, M. Sulanowska and P.A. Rona, Active vents and massive sulfides at 26° N (TAG) and 23° N (Snakepit) on the Mid-Atlantic Ridge, Can. Mineral. 26, 697–711, 1988.
12 A.C. Campbell, M.R. Palmer, G.P. Klinkhammer, T.S. Bower, J.M. Edmond, J.R. Lawrence, J.F. Casey, G. Thompson, S.E. Humphris, P.A. Rona and J.A. Karson, Chemistry of hot springs on the Mid-Atlantic Ridge: TAG and MARK sites, Nature 335, 514–519, 1988.
13 Scientific Party, Leg 106, Mid Atlantic bare-rock drilling and hydrothermal vents, Nature 321, 14–15, 1986.
14 Scientific Party, Leg 106, Drilling the Snakepit hydrothermal sulfide deposit on the Mid-Atlantic Ridge, Lat. 23° 22′ N, Geology 14, 1004–1007, 1986.
15 C. Mevel, J.M. Auzende, M. Cannat, J.P. Donval, J. Dubois, Y. Fouquet, P. Gente, D. Grimaud, J.A. Karson, M. Segonzac and M. Stievenard, La ride du Snakepit (dorsale médio-Atlantique 23° 22′ N): résultats préliminaires de la campagne Hydrosnake, C.R. Acad. Sci. Paris 308, 545–552, 1989.
16 C. Lalou and E. Brichet, On the isotopic chronology of submarine hydrothermal deposits, Chem. Geol. (Isot. Geosci. Sect.) 65, 197–207, 1987.
17 C.W. Blount and F.W. Dickson, The solubility of anhydrite ($CaSO_4$) in NaCl-H_2O from 100 to 450° C and 1 to 1000 bars, Geochim. Cosmochim. Acta 33, 227–245, 1969.
18 C. Lalou and E. Brichet, Possibilité de datation des dépôts de sulfures métalliques hydrothermaux sous marins par les descendants à vie courte de l'uranium et du thorium, C.R. Acad. Sci. Paris, Sér. II 293, 821–826, 1981.
19 C. Lalou, E. Brichet and R. Hekinian, Age dating of sulfide deposits from axial and off-axial structures of the East Pacific Rise near 12° 50′ N, Earth Planet. Sci. Lett. 75, 59–71, 1985.
20 V. Marchig, H. Rosch, C. Lalou, E. Brichet and E. Oudin, Zonation in a large sulfide chimney from the East Pacific Rise at 18° S: relations with its chronological built up, Can. Mineral. 26, 541–554, 1988.
21 C. Lalou and E. Brichet, Age and implication of East Pacific Rise sulfide deposits at 21° N, Nature (London) 300, 169–171, 1982.
22 C. Lalou, E. Brichet and J. Lange, Fossil hydrothermal sulfide deposits at the Galapagos spreading center near 85° 00 West: geological setting, mineralogy and chronology, Oceanol. Acta 21(1), 1–8, 1989.
23 C. Lalou, E. Brichet, T.L. Ku and C. Jehanno, Radiochemical, scanning electron microscope (SEM) and X ray dispersive energy (EDAX) studies of a FAMOUS hydrothermal deposit, Mar. Geol. 24, 245–258, 1977.
24 C. Lalou, E. Brichet, C. Jehanno and H. Perez-Leclaire, Hydrothermal manganese deposits from Galapagos mounds DSDP Leg 70 Hole 529B and Alvin dives 729 and 721, Earth Planet. Sci. Lett. 63, 63–75, 1983.
25 J.L. Reyss, N. Lemaitre, P. Bonte and D. Franck, Anomalous $^{234}U/^{238}U$ ratios in deep sea hydrothermal deposits, Nature 325, 798–800, 1987.
26 P.A. Rona, R.N. Harbison, B.G. Bassinger, R.B. Scott and A.J. Nalwalk, Tectonic fabric and hydrothermal activity of Mid-Atlantic Ridge crest (Lat. 26° N), Geol. Soc. Am. Bull. 87, 661–674, 1976.
27 P.A. Rona and D.F. Gray, Structural behavior of fracture zones symmetric and asymmetric about a spreading axis: Mid-Atlantic Ridge (Latitude 23° N to 27° N), Geol. Soc. Am. Bull. 91, 485–494, 1980.
28 S. Metz, J.H. Trefry and T.A. Nelsen, History and geochemistry of a metalliferous sediment core from the Mid-Atlantic Ridge at 26° N, Geochim. Cosmochim. Acta 52, 2369–2378, 1988.
29 G. Thompson, A geochemical study of some lithified carbonates from the deep sea, Geochim. Cosmochim. Acta 36, 1237–1253, 1972.
30 J.H. Natland, Basal ferromanganoan sediments at DSDP site 183, Aleutian Abyssal Plain, and site 192, Meiji guyot, Northwest Pacific, Leg 19, Init. Rep. DSDP XIX, 15, 629–636, 1973.
31 J.L. Gevirtz and G.M. Friedman, Deep sea carbonate sediments of the Red Sea and their implications on marine lithification, J. Sediment. Petrol. 36, 143, 1966.
32 E.J. Zeller and J.L. Wray, Factors influencing precipitation of calcium carbonate, Am. Assoc. Pet. Geol. Bull. 40, 140–148, 1956.
33 J.L. Wray and F. Daniels, Precipitation of calcite and aragonite, J. Am. Chem. Soc. 79, 274–280, 1957.
34 T. Tarutani, R.N. Clayton and T.K. Mayeda, The effect of polymorphism and magnesium substitution on oxygen isotope fractionation between calcium carbonate and water, Geochim. Cosmochim. Acta 33, 987–996, 1969.
35 E.L. Grossman and T.L. Ku, Oxygen and carbon isotope fractionation in biogenic aragonite: temperature effects, Chem. Geol. (Isot. Geosci. Sect.) 59, 59–74, 1986.
36 J.R. Lawrence and J.I. Drever, Evidence for cold water circulation at DSDP site 395: isotopes and chemistry of alteration products, J. Geophys. Res. 86(B6), 5125–5133, 1981.
37 D.G. Temple, R.B. Scott and P.A. Rona, Geology of a

submarine hydrothermal field, Mid-Atlantic Ridge 26° N latitude, J. Geophys. Res. 84, 7453–7466, 1979.

38 J.A. Karson and P.A. Rona, Block-tilting, transfer faults and structural control of magmatic and hydrothermal processes in the TAG area, Mid-Atlantic Ridge 26° N, Geol. Soc. Am. Bull., in press, 1989.

39 L.P. Zonenshain, M.I. Kuzmin, A.P. Lisitsin, Yu.A. Bogdanov and B.V. Baranov, Tectonics of the Mid-Atlantic rift valley between the TAG and MARK areas (26–24° N): evidence for vertical tectonism, Tectonophysics 159, 1–23, 1989.

40 J.M. Edmond, K.L. Von Damm, R.E. McDuff and C.I. Measures, Chemistry of hot springs on the East Pacific Rise and their effluent dispersal, Nature 297, 187–191, 1981.

41 C. Lalou, E. Brichet and H. Perez-LeClaire, The Galapagos hydrothermal mounds history from about 600,000 years to Present, Oceanol. Acta 7(3), 261–270, 1984.

42 J.A. Karson, G. Thompson, S.E. Humphris, J.M. Edmond, W.B. Bryan, J.R. Brown, A.T. Winters, R.A. Pockalni, J.F. Casey, A.C. Campbell, G. Klinkhammer, M.R. Palmer, R.J. Kinzler and M. Sulanowska, Along axis variations in seafloor spreading in the MARK area, Nature 328, 681–685, 1987.

43 M. Stuiver and H.G. Ostlund, Radiocarbon Atlantic, Radiocarbon 22, 1–24, 1980.

44 M. Stuiver, G.W. Pearson and T. Brazivnas, Radiocarbon age calibration of marine samples back to 9000 years B.P., Radiocarbon 28, 980–1021, 1986.

45 M. Stuiver, B. Kromer, B. Becker and C.W. Ferguson, Radiocarbon calibration back to 13,300 years B.P., Radiocarbon 28, 969–979, 1986.